

## Dissipative factors in the free-decay behaviour of an Oscillating Water Column

R. Manasseh<sup>1</sup>, L. Puticiu<sup>1</sup>, Md. K. Hasan<sup>1</sup> and J. Leontini<sup>1</sup>

<sup>1</sup>Department of Mechanical & Product Design Engineering  
Swinburne University of Technology, Hawthorn, VIC 3122  
Melbourne, Australia

### Abstract

Experimental data on the free decay of water oscillating in a partially-submerged tube are presented, and are compared with simulations based on idealised ordinary differential equation models. The aim was to study the significance of the dissipative terms causing the free decay of the motion of the water column released from an elevated initial condition. It was found that the overall damping could be approximated with linear damping ratios between approximately 0.04 and 0.06, with standard deviations of the damping ratios generally 5-10%.

### Introduction

A partially-submerged vertical-axis tube fixed in inertial space provides the most elementary model for the Oscillating Water Column (OWC), the oldest-established concept for extracting renewable energy from ocean waves. The OWC is also of interest for infrastructure that could protect vulnerable coastlines from waves.

A number of OWC designs have been realised and installed in the ocean since 1885, and a number have been grid-connected [8]. In coastal-protection context, the breakwater-OWC plant at Mutriku, Spain [15] is presently delivering power to the grid as well as protecting a port from ocean waves.

In the present experiments, the OWC is simply a tube open at both ends, with the bottom of the tube immersed such that a length  $L$  is underwater (Fig. 1). The top of the column is in the air. In full-scale OWC designs, the part of the tube in the air communicates with the atmosphere via a turbine such as the Wells turbine. Such turbines are able to rotate in the same direction in both the upwards and downwards motion of air driven by the rising and falling water column, at the expense of lower efficiency than conventional turbines [5].

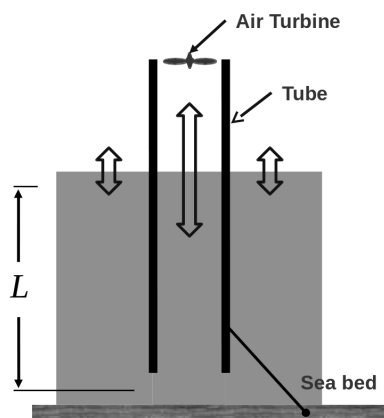


Figure 1: Schematic of a generic OWC. In practice, most OWCs would have a 'bent' duct such that the total length of underwater tube is  $L$ , but the principle is identical.

The essential physics of the OWC can be understood from a simple application of Newton's Second Law, before considering any fluid dynamics. This shows that when the water inside the tube is displaced infinitesimally from rest, in a 'piston-like' motion such that the free surface remains flat, the column of water is an oscillator with natural frequency  $\omega_0 = \sqrt{g/L}$ , where  $g$  is the acceleration due to gravity. In this elementary approximation, the OWC is a 'liquid pendulum' [12].

Like the majority of wave-energy converter concepts, the OWC is designed to be a resonator: the natural frequency  $\omega_0$  is 'tuned' to be similar to the dominant frequency of the ocean swell, essentially by fixing  $L$  at the design stage. The advantage of resonance is that the machine, whatever its type, moves with a larger amplitude than the surrounding water, representing energy extraction from the ocean over a volume much larger than the machine's physical size [12]. While the tuning is easily accomplished by designing the tube to have the correct submerged length  $L$ , knowledge of the amplitude of water oscillation inside the tube is critically important since the amplitude defines the amount of energy extracted from the waves. The amplitude would be predictable if the equivalent of a linear damping ratio were known. However, the dissipative factors giving the damping are challenging to predict, because resonance implies large amplitude, and large amplitude implies nonlinearity.

This paradox of resonant wave-energy conversion - that the design is based on linear theory but nonlinearity is desired - is recognised as an issue by the wave-energy community [14]. In experiments on a laboratory scale model of a commercial OWC, Fleming et al. [6] pointed out that two dissipative factors would be due to nonlinear processes: turbulent losses, and vortex formation at the mouth of the device. However, it was noted that it would be difficult to ascribe experimentally-measured energy losses to specific processes [6]. Linear wave physics causes damping of the motion owing to wave radiation, and the internal boundary layers also cause linear damping if they are laminar. However, an interesting fundamental issue with OWCs is that the internal boundary layers can undergo a 'conditional' transition to turbulence, a phenomenon noted in reciprocating pipe flow [1], but otherwise little-studied [7]. In conditional turbulence, the flow is laminar when the oscillation cycle is around zero velocity, then a transition to turbulence occurs during the deceleration phase, followed by re-laminarisation [17]. Up to 50% of the cycle could be laminar, even at oscillatory Reynolds numbers typical of full-scale OWCs [1].

Vortex formation is a further nonlinear phenomenon. Initial estimates of the nonlinearity due to the displacement of water in a highly idealised OWC, plus the turbulent boundary-layer dissipation, suggested that these two forms of nonlinearity could significantly reduce power output [10]. Preliminary theoretical and numerical studies suggested that once vortex-formation losses were included, they could reduce power output of an OWC by 45% under realistic ocean conditions [11].

The aim of the present paper is to make a first comparison between the experimentally-measured damping of an OWC and

a simplified ordinary differential equation model of the one-dimensional dynamics. The objective is to determine which of the dissipative terms is most important. The experiment studied the free decay of an OWC from a fairly large initial displacement from rest. A free-decay experiment has the advantage that it is possible to study the behaviour in any tank large enough such that reflections of waves from the walls would be small. There need not be a wave-making mechanism. It is also easy to extract a damping ratio from the data, although that is an inherently linear concept. A disadvantage is that the nonlinearity is large at the start (for a large initial displacement) but decreases with each cycle, which is not representative of the forced case of real ocean-driven OWCs.

## Experimental method

### Apparatus

Experiments were performed in a  $6.7 \times 3.7$  m tank 1.3 m deep filled with water to a depth of 0.8 m. Clear-acrylic tubes formed the oscillating water columns. The columns were 900 mm long and all had the same surface roughness determined by the manufacturing process of acrylic tubes. The outside diameters were 30, 35, 50, 60 and 100 mm and the tube-wall thickness was approximately 2 mm. The columns were clamped at various submergence depths from a rigid frame above the tank.

The top end of the column was sealed with a rubber lid. A vacuum pump was connected to the part of the column in the air via a 3 mm hose. A weight ensured the lid was sealed completely under vacuum while keeping it easy to remove.

To permit video tracking of the water-surface displacement, a float about 30 mm long and 10 mm in diameter was placed inside the column. A lightweight antenna was fitted to the top of the float while a small mass (a few grams) at its bottom kept it upright. The top of the antenna was fitted with a 3-mm diameter light cloth sphere fitted with fine spikes. The spikes ensured that whenever the float came too close to the walls of the column, friction was minimal, resulting in the cloth sphere having a vertical displacement as close as practical to that of the water surface, while being sufficiently clear of the external water level to permit clear tracking of the displacement.

The water-column surface was elevated with the vacuum pump to achieve the desired initial displacement, which was held in place with a one-way valve on the 3 mm hose. The rubber lid was attached via a wire and pulley to a weight. Once the weight was allowed to fall, the lid was quickly removed, exposing the entire diameter of the top of the tube to atmospheric pressure at time  $t = 0$ . Tests confirmed that this release method resulted in repeatable data.

Experiments were repeated 35-40 times with a three-minute delay between runs, which was more than sufficient for all water motion to have died away.

### Data acquisition

The movement of the cloth sphere was tracked using a Sony HDR-AS15 water-resistant action camera at 120 fps in 720p quality. The videos were digitised (Tracker version 4.95, Brown, D, Open Source Physics).

This free-decay approach meant that the reciprocating flow was initially highly nonlinear, then decayed to linear-dominated behaviour. Data were disregarded after surface waves reflected from the walls would have returned to the tube, typically allowing 5-10 complete cycles of data.

Periods measured from the videos never included the initial dis-

placement peak. The 95% confidence interval on the oscillation period (under 0.012 seconds) was found to be within the resolution of the time sampling interval (0.025 seconds).

## Semi-analytic modelling of OWC dynamics

The ‘loss’ of energy from a wave-energy converter is usually represented by radiation of waves to infinity, modelled using potential flow (e.g. [3, 13].) The theoretical basis is outlined elsewhere [2, 11].

Of course, in practice the machine would have a power take-off (usually some form of electrical generator), but in the experiments to be modelled, this was absent.

To express the ‘piston mode’ of the OWC that is not driven and simply relaxes from an initial displacement, the Navier-Stokes equations are integrated over the duct cross-section and along the submerged duct length [9, 7]. As in [9], this reduces the momentum balance to an ordinary differential equation in the vertical displacement of the free surface. Introducing the scalings  $X_0$  for length, where  $X_0$  is the initial displacement, and  $\omega_0^{-1}$  for time, leads to a momentum balance in the non-dimensional vertical displacement of the free surface,  $\xi$ ,

$$(1 + a_\mu)(1 + \varepsilon\xi)\ddot{\xi} + 2\zeta_\mu\dot{\xi} + \varepsilon C_e|\dot{\xi}|\dot{\xi} + \varepsilon C_f|\dot{\xi}|^{3/4}\dot{\xi} + \xi = 0, \quad (1)$$

where  $a_\mu$  is the added mass due to radiation,  $\zeta_\mu$  is the linear damping,  $\varepsilon = X_0/L$ , and  $C_e$  and  $C_f$  are the nonlinear damping co-efficients due to free-end effects and internal turbulent boundary layers, respectively. There is a nonlinear inertia,  $\varepsilon\xi\ddot{\xi}$ , which arises from the mass of water in the column varying with displacement, and two nonlinear dissipation terms,  $\varepsilon C_f|\dot{\xi}|^{3/4}\dot{\xi}$  and  $\varepsilon C_e|\dot{\xi}|\dot{\xi}$ . A survey of reciprocating turbulence literature [7] suggests the best model for  $C_f$  is given by the correlation of Akhavan et al [1],

$$C_f = 0.15816 \text{Re}_\omega^{-1/4}, \quad (2)$$

where the oscillatory or ‘kinetic’ Reynolds number is given by  $\text{Re}_\omega = \omega D^2/\nu$ , with  $D$  being the diameter of the tube and  $\nu$  the kinematic viscosity. This assumes the flow is fully developed in a ‘pipe-like’ OWC duct. Despite the likelihood of conditional turbulence [1], the ‘worst case’ was assumed in which the flow was 100% turbulent; as found in earlier studies [7, 11], boundary-layer dissipation is comparatively small. The value of  $C_e$  represents the cycle-averaged dissipative loss due to the formation of underwater vortices at the mouth of the OWC. It was parameterised from Direct Numerical Simulations (DNS) of a tube driven in reciprocating flow, as detailed in [7] and [11]. The use of a cycle-averaged term parameterised from constant-forcing-amplitude DNS may be inappropriate for the free-decay case, since the ‘amplitude’ is constantly varying in free decay; however, this is the only parameterisation available at present.

The parameter  $\varepsilon$  would be very small for initial displacements  $X_0$  that are very small relative to the submerged length  $L$ , linearising the system. However, the value of  $\varepsilon$  is 0.35 for the present experiment, representing moderate nonlinearity. The linear damping ratio  $\zeta_\mu$  is assumed to be entirely due to radiation damping and it can be calculated from theoretical analyses of OWCs (e.g. [4, 7]). For the experimental cases to be modelled, it takes values from about 0.0005 to 0.0070, representing quite small damping due to wave radiation in the actual experimental system used. The added mass is determined from the same analysis as the radiation damping, since they form the one complex number; it can be assumed absorbed into a modified natural frequency following the same assumption that the radiation damping is frequency-invariant.

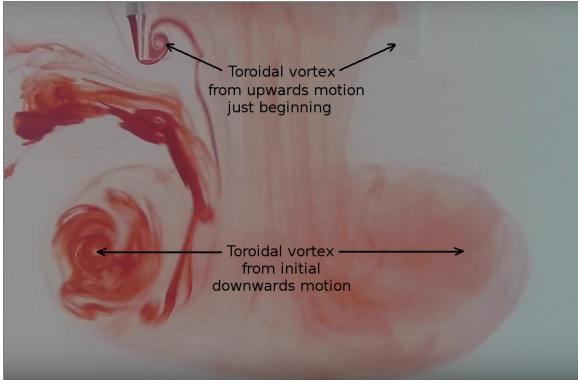


Figure 2: Flow-visualisation laboratory experiment on the free decay of an oscillating water column of 0.096 m diameter. Image (at about  $t = 2$  s) is just after the maximum downwards displacement during the first cycle after release, so that upwards flow has just begun.

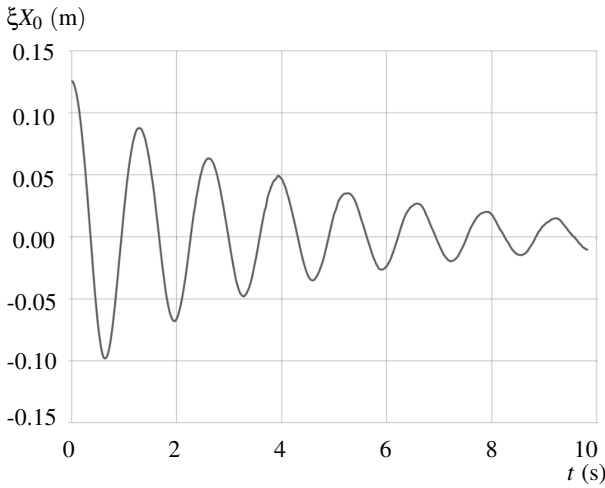


Figure 3: Example of an experimental time series of the water-surface elevation inside a column of internal diameter  $D = 0.031$  m, with a submerged depth of 0.4 m and an initial displacement  $X_0 = 0.14$  m (occurring slightly before  $t = 0$ ).

### Numerical method

In the present paper, (1) is simply integrated in time to determine a nonlinear response. A fixed-timestep Runge-Kutta method was used. Peaks in the response were identified exactly as for the experiment, and fitted to determine a damping ratio. Of course, this forces a linear concept onto an inherently nonlinear system, but will be seen shortly, the experimental response does fit an exponential-decay model quite well.

### Results

A flow visualisation of one of the runs is shown in Fig. 2. As noted above, about 5-10 oscillation cycles could be resolved before waves would have hit the side walls and would have reflected back to the OWC. A typical timeseries is shown in Fig. 3. Despite the initial displacement of  $X_0 = 0.14$  m being 0.35 of the tube length  $L$  (hence  $\epsilon = 0.35$ ), the decay appears quasi-exponential, as if the behaviour were linear. The loci of the peaks (and of absolute values of the troughs) of the surface elevation were fitted by exponentials as shown in Fig. 4, where the curves for five different OWC diameters are shown.

Simulated timeseries show exponentially-decaying behaviour

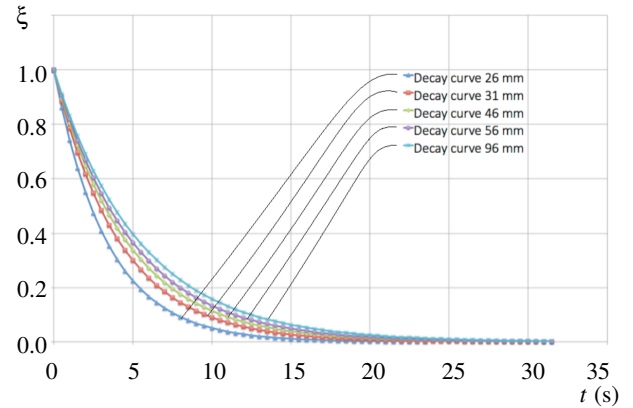


Figure 4: Experimental decay curves for five oscillating water columns with different internal diameters  $D$ ; all had a submerged depth of 0.4 m and were given an initial displacement of 0.14 m, normalised to  $\xi = 1$  here.

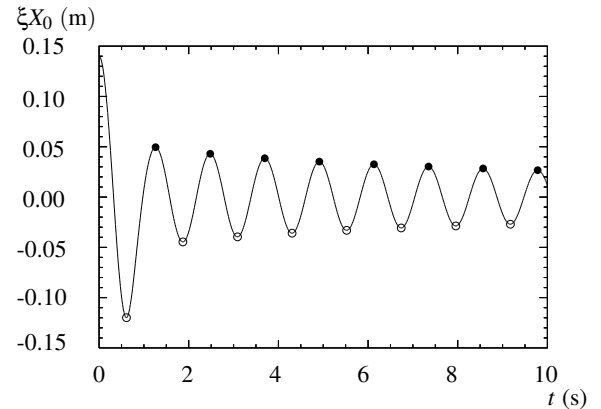


Figure 5: Simulated time series for the parameters of figure 3 ( $D = 31$  mm), showing non-exponential behaviour for the first two cycles. For values of  $D$  greater than 0.031 m, simulated results appeared to decay exponentially, as in the experiment.

for  $D > 31$  mm, similar to the experiments. However, for the smaller diameters of  $D = 0.026$  and  $0.031$  m (figure 5), the drop in amplitude over the first two cycles is much more severe than the quasi-exponential behaviour of the remaining cycles.

From the experimental exponential fits, the damping ratio for each case can be extracted, together with 95% confidence limits on these values, as shown in Fig. 6. Standard deviations of the damping ratios were generally 5-10%, and with a large number of runs, the confidence limits were small.

It can be seen that the experimental damping ratios  $\zeta$  (filled symbols) decrease with increasing tube diameter, being approximately 0.06 for a 0.026 m tube and approximately 0.04 for a 0.096 m tube.

The simulation results are also shown on Fig. 6 (open symbols). In these calculations, all the terms in (1) were present. It is clear that the same trend of decreasing damping with increasing diameter is observed. However, the simulations overpredict the damping for small diameters and underpredict the damping for large diameters. The dissipation terms could be selectively

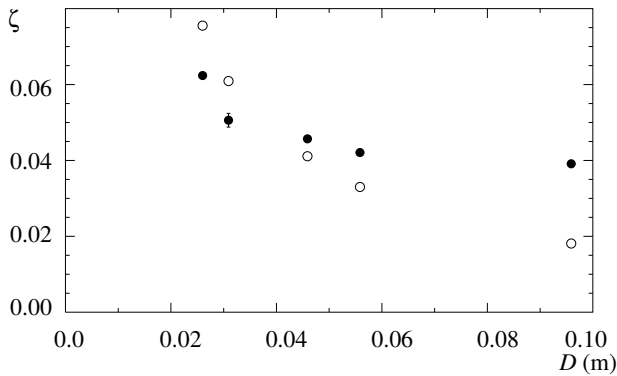


Figure 6: Experimental damping ratios  $\zeta$  for five oscillating columns with different internal diameters  $D$  (filled symbols), compared with the results of integrating the corresponding ODEs (open symbols). All cases were at a submerged depth of 0.4 m and were given an initial displacement of 0.14 m. Experimental error bars are only larger than the symbol in one case ( $D = 0.031$  m) and represent 95% confidence limits based on repeated experiments.

turned off in the calculation. Very little difference was achieved by removing the boundary-layer dissipation term, but removing the vortex-formation dissipation term resulted in damping ratios very significantly below the experimental values, demonstrating that most of the simulated dissipative loss was due to the parameterised vortex formation term.

### Conclusions

Experiments on the free decay of an elementary Oscillating Water Column showed that despite the formation of large vortices at the mouth of the column on each downstroke, the overall decay rate of the water-surface elevation appeared remarkably linear. Linear damping ratios extracted from the experimental data were approximately 0.04 to 0.06.

An attempt was made to understand the sources of dissipation causing the decay, since such an understanding would assist engineering-design decisions. Analytically-derived damping due to radiation of waves - a linear effect - was small. The first nonlinear dissipative term, internal boundary-layer friction, even assuming the flow was fully turbulent throughout the cycle, likewise made a small contribution. The dominant contribution to dissipation was another nonlinear effect, the formation of vortices at the end. This is curious, since the experimental outcome of this highly nonlinear process is what appears to be a quasi-exponential decay typical of linear processes. The cycle-averaged vortex loss yielded overall damping ratios with the same general trend as the experimental data. However, for the smaller diameters, the initial drop was too severe, suggesting the cycle-averaging was inappropriate. Future work should focus on a better parameterisation of the formation of vortices.

### Acknowledgements

Aspects of the analytic work were funded by the Australian Renewable Energy Agency under grant ERP A00575.

### References

[1] Akhavan, R., Kamm, R. and Shapiro, A., An investigation of transition to turbulence in bounded oscillatory Stokes flows. part 1. experiments, *Journal of Fluid Mechanics*, **225**, 1991, 395–422.

[2] De Chowdhury, S. and Manasseh, R., Behaviour of eigenmodes of an array of oscillating water column devices, *Wave Motion*, **74**, 2017, 56–72.

[3] Evans, D., Wave-power absorption by systems of oscillating surface pressure distributions, *Journal of Fluid Mechanics*, **114**, 1992, 481–499.

[4] Evans, D. and Porter, R., Efficient calculation of hydrodynamic properties of OWC-type devices, *Journal of Offshore Mechanics and Arctic Engineering*, **119**, 1997, 210–218.

[5] Falcão, A. F. O., Wave energy utilization: A review of the technologies, *Renew. Sust. Energy Rev.*, **14**, 2010, 899–918.

[6] Fleming, A., Peneisis, I., MacFarlane, G., Bose, N. and Denniss, T., Energy balance analysis for an oscillating water column wave energy converter, *Ocean Eng.*, **54**, 2012, 26–33.

[7] Hasan, M. K., *Dissipation in Oscillating Water Columns*, Ph.D. thesis, Swinburne University of Technology, 2017.

[8] Heath, T., A review of oscillating water columns, *Philosophical Transactions of the Royal Society A: Mathematical, Physical and Engineering Sciences*, **370**, 2012, 235–245.

[9] Illesinghe, S., Hasan, M. K. and Manasseh, R., Multiphase dynamics of oscillating-water-column ocean wave energy converters, 18th Australasian Fluid Mechanics Conference, Launceston, Australia, 3-7 December 2012, paper 371, 2012.

[10] Manasseh, R., Hasan, M. K. and De Chowdhury, S., Non-linear behaviour of interacting oscillating water columns, Proceedings, 20th Australasian Fluid Mechanics Conference, Perth, Australia, 5–8 December, 2016.

[11] Manasseh, R., Hasan, M. K., Leontini, J. S., Puticiu, L. and De Chowdhury, S., Effects of machine nonlinearity on the performance of idealised wave-energy converters, Proceedings, 12th European Wave and Tidal Energy Conference, Cork, Ireland, 27–31 August, 2017, 2017.

[12] Manasseh, R., McInnes, K. and Hemer, M., Pioneering developments of marine renewable energy in Australia, *Int. J. Ocean & Climate Systems*, **8**, 2017, 50–67.

[13] Nader, J.-R., Zhu, S.-P., Cooper, P. and Stappenbelt, B., A finite-element study of the efficiency of arrays of oscillating water column wave energy converters, *Ocean Engineering*, **43**, 2012, 72–81.

[14] Spanos, P., Arena, F., Richichi, A. and Malara, G., Efficient dynamic analysis of a nonlinear wave energy harvester model, *ASME. J. Offshore Mech. Arct. Eng.*, **138**, 2016, 041901–041901–8.

[15] Torre-Enciso, Y., Marqués, J. and Marina, D., Mutriku: First year review, 4th International Conference on Ocean Energy, 17-19 October, Dublin, 2012.

[16] Wolgamot, H., Effects of second-order hydrodynamics on efficiency of a wave energy array, 11th European Wave and Tidal Energy Conference, Nantes, France, 6–11 September 2015, 2015.

[17] Zhao, T. and Cheng, P., The friction coefficient of a fully developed laminar reciprocating flow in a circular pipe, *Int. J. Heat and Fluid Flow*, **17**, 1996, 167–172.